Plasmodium vivax spleen-dependent genes encode antigens associated with cytoadhesion and clinical protection

Carmen Fernandez-Becerra[a,b,1], Maria Bernabeu[a,2], Angélica Castellanos[c], Bruna R. Correa[d,3], Thomas Obadia[e], Miriam Ramirez[a], Edmilson Rui[a], Franziska Hentzschel[a,4], Maria López-Montañés[a], Alberto Ayllon-Hermida[a], Lorena Martin-Jaular[a,5], Aleix Elizalde-Torrent[a,6], Peter Siba[f], Ricardo Z. Vêncio[d], Myriam Arevalo-Herrera[c], Sócrates Herrera[c], Pedro L. Alonso[a,7], Ivo Mueller[e,g], and Hernando A. del Portillo[a,b,h,1]

[a]ISGlobal, Hospital Clínic, Universitat de Barcelona, Barcelona 08036, Spain; [b]Institut d'Investigació Germans Trias i Pujol, Badalona 08916, Spain; [c]Centro de Investigación Científica Caucaseco, Cali, Valle, Colombia [d]Department of Computing and Mathematics FFCLRP, Ribeirao Preto, Universidade de São Paulo, São Paulo 14040-900, Brazil; [e]Department of Parasites and Insect Vectors, Institut Pasteur, Paris 75015, France; [f]Papua New Guinea Institute of Medical Research, Madang, Papua New Guinea; [g]Population Health and Immunity Division, The Walter and Eliza Hall Institute of Medical Research, Parkville, VIC 3052, Australia; and [h]Institució Catalana de Recerca I Estudis Avançats, Barcelona 08010, Spain

Edited by Louis H. Miller, National Institute of Allergy and Infectious Diseases, NIH, Rockville, MD, and approved April 16, 2020 (received for review November 23, 2019)

***Plasmodium vivax*, the most widely distributed human malaria parasite, causes severe clinical syndromes despite low peripheral blood parasitemia. This conundrum is further complicated as cytoadherence in the microvasculature is still a matter of investigations. Previous reports in *Plasmodium knowlesi*, another parasite species shown to infect humans, demonstrated that variant genes involved in cytoadherence were dependent on the spleen for their expression. Hence, using a global transcriptional analysis of parasites obtained from spleen-intact and splenectomized monkeys, we identified 67 *P. vivax* genes whose expression was spleen dependent. To determine their role in cytoadherence, two *Plasmodium falciparum* transgenic lines expressing two variant proteins pertaining to VIR and Pv-FAM-D multigene families were used. Cytoadherence assays demonstrated specific binding to human spleen but not lung fibroblasts of the transgenic line expressing the VIR14 protein. To gain more insights, we expressed five *P. vivax* spleen-dependent genes as recombinant proteins, including members of three different multigene families (VIR, Pv-FAM-A, Pv-FAM-D), one membrane transporter (SECY), and one hypothetical protein (HYP1), and determined their immunogenicity and association with clinical protection in a prospective study of 383 children in Papua New Guinea. Results demonstrated that spleen-dependent antigens are immunogenic in natural infections and that antibodies to HYP1 are associated with clinical protection. These results suggest that the spleen plays a major role in expression of parasite proteins involved in cytoadherence and can reveal antigens associated with clinical protection, thus prompting a paradigm shift in *P. vivax* biology toward deeper studies of the spleen during infections.**

Plasmodium vivax | spleen-dependent genes | cytoadherence | global transcription

Human malaria caused by *Plasmodium vivax* infection (vivax malaria) is a major global health issue. It is the most geographically widespread form of the disease, accounting for 7.5 million annual clinical cases, the majority of cases in America and Asia, and estimation of over 2.5 billion people living under risk of infection (1). The general perception toward vivax malaria has shifted recently, following a series of reports, from being viewed as a benign infection to the recognition of its potential for more severe manifestations, including fatal cases (2–4). However, the underlying pathogenic mechanisms of vivax malaria remain largely unresolved.

Central to the pathology in *Plasmodium falciparum*, the most virulent malaria-causing human species, is the phenomenon of cytoadherence to endothelial receptors mediated by variant surface proteins that facilitate sequestration of parasitized red blood cells (RBCs) deep in microvasculature (5). The absence of mature parasites in peripheral blood of patients is unequivocal evidence of cytoadherence and parasite sequestration in this species. In contrast,

Significance

In spite of low peripheral blood parasitemia, vivax malaria causes severe disease. This conundrum finds an explanation from reports suggesting that the spleen is a place for parasite sequestration. We performed a global transcriptional analysis of parasites that grew in the presence or absence of the spleen in a nonhuman primate model. We identified 67 spleen-dependent genes, including multigene variant families, and functionally demonstrated specific adherence to human spleen fibroblasts by a member of such families. Moreover, we further demonstrated that spleen-dependent *Plasmodium vivax* genes code for immunogenic proteins during natural infections. Our results indicate that this organ plays an important function in *P. vivax* malaria and call for deeper studies of the role of spleen in *P. vivax* infections.

Author contributions: C.F.-B., M.B., B.R.C., L.M.-J., R.Z.V., M.A.-H., S.H., P.L.A., I.M., and H.A.d.P. designed research; C.F.-B., M.B., A.C., M.R., E.R., F.H., M.L.-M., L.M.-J., A.E.-T., and H.A.d.P. performed research; P.S. contributed new reagents/analytic tools; C.F.-B., M.B., B.R.C., T.O., A.A.-H., R.Z.V., M.A.-H., S.H., I.M., and H.A.d.P. analyzed data; and C.F.-B. and H.A.d.P. wrote the paper.

The authors declare no competing interest.

This article is a PNAS Direct Submission.

Data deposition: All data are freely available through the Gene Expression Omnibus database, https://www.ncbi.nlm.nih.gov/geo (accession no. GPL6667).

[1]To whom correspondence may be addressed. Email: carmen.fernandez@isglobal.org or hernandoa.delportillo@isglobal.org.

[2]Present address: European Molecular Biology Laboratory, Barcelona 08003, Spain.

[3]Present address: Centre for Genomic Regulation, The Barcelona Institute of Science and Technology, Barcelona, Catalonia 08003, Spain.

[4]Present address: Wellcome Centre for Integrative Parasitology, Institute of Infection, Immunity and Inflammation, University of Glasgow, Glasgow 120, United Kingdom.

[5]Present address: INSERM U932, Institut Curie Centre de Recherche, PSL Research University, Paris 75005, France.

[6]Present address: IrsiCaixa AIDS Research Institute, Hospital Germans Trias in Pujol, Badalona, Catalonia 08916, Spain.

[7]Present address: World Health Organization, Geneva 1211, Switzerland.

This article contains supporting information online at https://www.pnas.org/lookup/suppl/doi:10.1073/pnas.1920596117/-/DCSupplemental.

First published May 21, 2020.

as infected reticulocytes with mature stages of *P. vivax* are detected in peripheral circulation, for a long time it was amply accepted that this human malaria parasite does not sequester in the microvasculature. Against this dogma, in the last decade, different reports have described in vitro cytoadherence of *P. vivax*-infected reticulocytes to human cells and tissue cryosections (6–8). Moreover, infected reticulocytes were able to cytoadhere under static and flow conditions to cells expressing ICAM-1, a well-known *P. falciparum* receptor, and this binding was partly mediated by VIR proteins (6), a superfamily of variant surface proteins likely

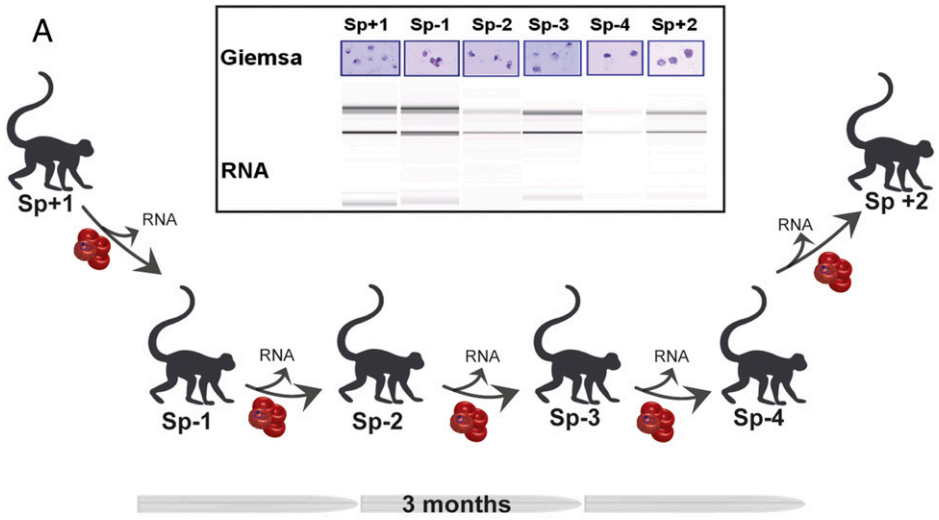

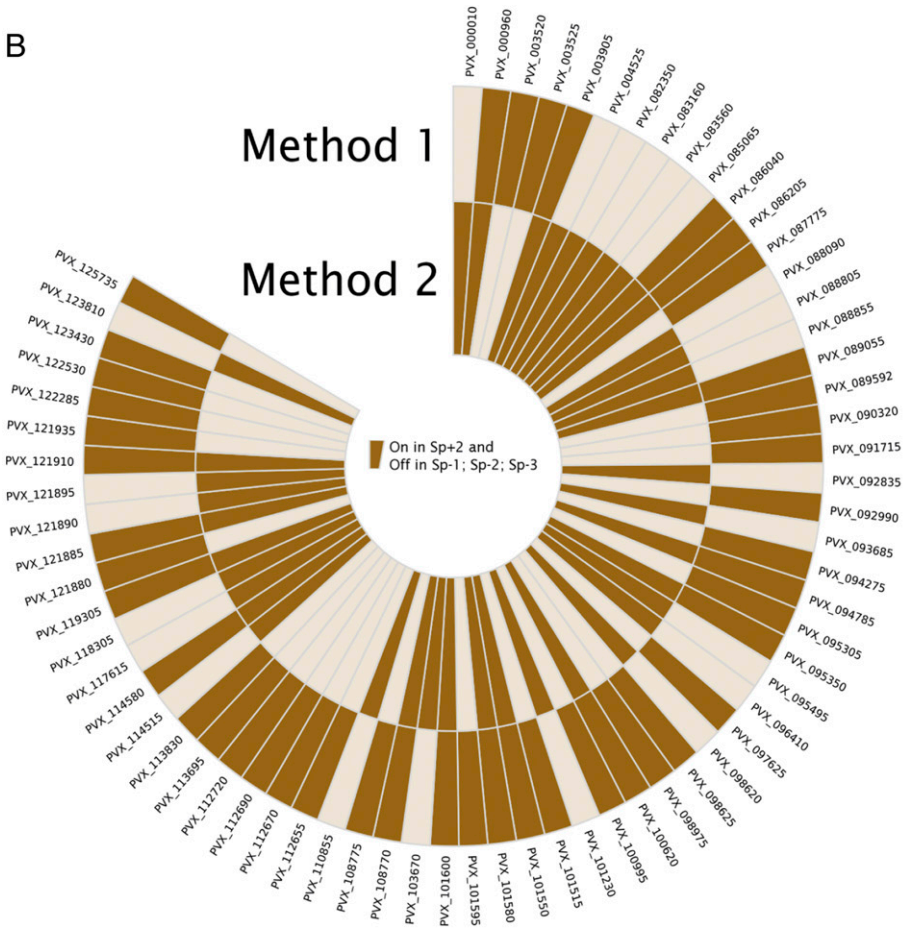

Fig. 1. Identification of *P. vivax* spleen-dependent genes. (*A*) Scheme of experimental infections and biological samples used for expression analysis. (*B*) Diagram showing genes only expressed in Sp+2 and negative in the splenectomized monkeys for any of the two algorithms used.

involved in cytoadherence (9, 10). Therefore, even though the exact molecular mechanisms of cytoadherence are not fully elucidated, these observations prompt a paradigm shift in *P. vivax* biology.

Malaria parasites infections induce a dramatic splenic response mostly characterized by variable levels of splenomegaly. This is probably due to the fact that the spleen plays an important dual role in malaria: destruction of infected red blood cells (iRBCs) and expression of parasite antigens, including variant surface proteins involved in pathology (11, 12). Thus, pioneering experiments with *Plasmodium knowlesi* parasites obtained from splenectomized monkeys showed that parasites no longer expressed variant antigens (SICA) on the surface of iRBCs and that immune sera from these animals failed to agglutinate iRBCs with mature stages (13). Upon passage of these parasites into monkeys with intact spleens, however, parasites recovered the expression of SICA antigens, and immune monkey sera showed the agglutinating phenotype. In a more recent study, it has been demonstrated that the spleen plays an important role in controlling the transcriptional and posttranscriptional expression of SICAvar antigens (14). Similar observations on expression of variant proteins were also made in monkey models of *P. falciparum* (15) and *Plasmodium fragile* (16) as well as in a rodent *Plasmodium chabaudi* model (17). In *P. falciparum* splenectomized patients, iRBCs present low expression of surface variant proteins and appearance of mature stages in peripheral blood, likely due to an impairment of parasite tissue sequestration (18, 19). In addition, in immune (19) and nonimmune individuals (20, 21), the absence of the spleen results in increased disease severity.

Altogether, these data support a major role of the spleen in modulating the expression of variant virulent determinants in malaria involved in cytoadherence. We thus hypothesized that *P. vivax* coding genes whose expression is dependent on an intact spleen will allow the identification of antigens involved in spleen cytoadherence and pathogenesis; to test this hypothesis, we used a global transcriptional approach in experimental *P. vivax* infections of spleen-intact and splenectomized *Aotus* monkeys to identify genes whose expression is spleen dependent.

Results

Identification of *P. vivax* Coding Genes with Intact Spleen-Dependent Expression. To identify *P. vivax* genes whose expression is spleen dependent, a series of experimental infections with the *P. vivax*

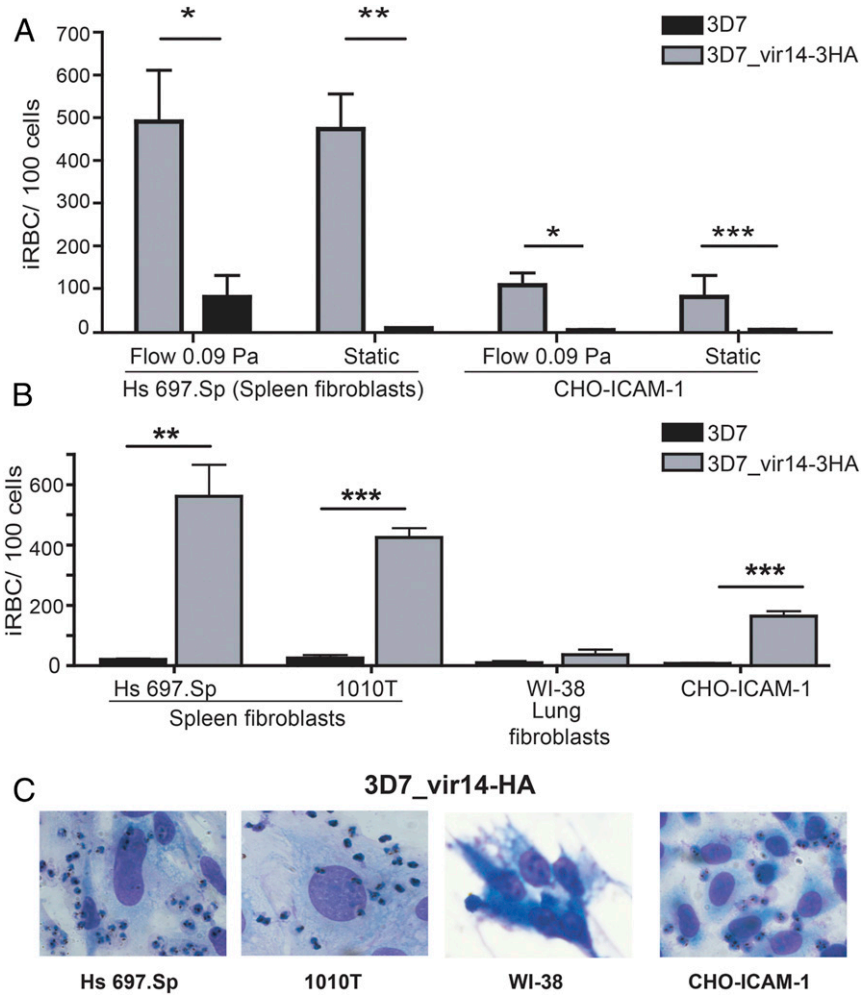

Fig. 2. VIR14 protein mediates adhesion to spleen fibroblasts. A *P. falciparum* transgenic line (3D7_vir14-3HA) previously reported to express VIR14 at the surface of iRBCs (23) showed cytoadhesion to spleen fibroblasts. Cytoadherence was expressed as iRBC per 100 cells. Significant higher binding than the *P. falciparum* 3D7 parental strain is represented with asterisks (unpaired *t* test). Results are shown as the mean of the binding ± SEM of three to five experiments. (*A*) Cytoadherence of 3D7 and the *P. falciparum* transgenic line 3D7_vir14-3HA to CHO-ICAM-1 cells and human spleen fibroblasts Hs 697.Sp under static and flow conditions at a wall shear stress of 0.09 Pa. (*B*) Cytoadherence of 3D7 and 3D7_vir14-3HA to CHO-ICAM-1 cells, lung fibroblasts WI-38, and spleen fibroblasts Hs 697.Sp and 1010T under static conditions. $*P < 0.05$; $**P < 0.01$; $***P < 0.005$. (*C*) Representative images of cytoadhesion of transgenic line 3D7_vir14-3HA to human spleen fibroblasts Hs 697.Sp (column 1) and 1010T (column 2), lung fibroblasts WI-38 (column 3), and CHO-ICAM-1 (column 4).

Salvador-1 (Sal-1) strain was performed in splenectomized (Sp−) and spleen-intact (Sp+) *Aotus* monkeys (Fig. 1*A*). After each infection, Giemsa smears were performed daily to determine the time to patency and peak of parasitemias (*SI Appendix*, Table S1). At peak parasitemias, mature parasites (multinuclei schizonts) were affinity purified (Fig. 1*A*). Although this purification step drastically reduced the total numbers of iRBCs, it was essential to achieve the highest level of comparability within the dataset. Dual hybridizations comparing the global expression of parasites obtained from the different experimental infections (labeled with Cy5) with a reference pool PvSp-1 obtained from splenectomized monkeys from the Centers for Disease Control and Prevention (CDC) donated by John Barnwell, Malaria Branch, Division of Parasitic Diseases and Malaria, CDC, Atlanta, GA (labeled with Cy3) were performed using an Agilent custom-made array containing 5,038 *P. vivax* coding genes (one 60-base oligonucleotide at every 2 kb) as annotated (10). Use of this reference pool from the CDC was needed due to the limited amounts obtained from our groups of monkeys Sp−1. Of note, sample Sp−4 was not included in these analyses due to insufficient amount of total RNA obtained. All data are freely available through the Gene Expression Omnibus (GEO) database (GEO accession no. GPL6667).

Two different statistical algorithms were used for expression analysis (*SI Appendix*, Fig. S1). In the first model, probe intensities were compared with negative controls. Average intensity of each probe was compared with the probability density function of the negative controls. If expression probability of negative controls was less than 0.001 compared with the probe, this probe was classified as "on." If it was greater than 0.05, probe was considered "off." In the second model, a 0.98 quantile of negative controls intensity was used as a cutoff. Probes presenting average intensity at least 10 times greater than this cutoff were considered on, and the ones with average intensity below the quantile were classified as off. For each model, selected genes were those presenting the following expression pattern: off in Sp−1, Sp−2, and Sp−3 and on in Sp+2. Using these criteria, a total of 67 spleen-dependent genes were identified, with close to 50% of them located in subtelomeric regions and around 26% in chromosome 14 (*SI Appendix*, Table S2). Genes could be grouped into those pertaining to multigene families, such as variant surface proteins (VIR) and *Pv-fam* genes. In addition, a high number of exported and hypothetical proteins and to a lesser extent, some enzymes and binding proteins were also identified (*SI Appendix*, Table S2).

VIR14 Protein Mediates Specific Adhesion to Human Spleen Fibroblasts. We have previously hypothesized that variant VIR proteins of *P. vivax* mediate cytoadherence to spleen barrier cells of fibroblastic origin (22). To test this hypothesis, we selected the PVX_108770 gene, encoding for VIR14, as its expression was predicted to be spleen dependent by two different algorithms (*SI Appendix*, Table S2). In the absence of long-term *P. vivax* in vitro culture, it had been previously used to generate a *P. falciparum* transgenic line (3D7_vir14-human influenza hemagglutinin [HA]) (23). In this transgenic line, VIR14 was localized at the surface of iRBC and showed cytoadhesion to CHO cells expressing the ICAM-1 receptor. To assess the cytoadhesion properties of this VIR protein to spleen fibroblasts, we first tested a commercial spleen fibroblast cell line, Hs 697.Sp (ATCC). This cell line was obtained from a patient who previously had a granulomatous lymph node and Hodgkin's disease without spleen involvement. Compared with the parental strain 3D7, cytoadherence of the transgenic line 3D7_vir14-3HA was significantly higher under flow and static conditions (Fig. 2 *A* and *C*). Moreover, adhesion to Hs 697.Sp was five times higher than the previously reported adhesion to CHO-ICAM-1 cells. To avoid confounding due to the pathogenic origin of cell line Hs 697.Sp, we generated a spleen fibroblast cell line (1010T) derived from a transplantation donor with a healthy spleen by culturing homogenized spleen cells for 3 wk. The transgenic strain 3D7_vir14-3HA also presented significantly higher adhesion to 1010T fibroblasts compared with the 3D7 parental strain (Fig. 2 *B* and *C*). To further determine the specificity of adhesion to spleen fibroblasts, static adhesion experiments were done using commercial lung fibroblasts (WI-38). No significant adhesion of the transgenic line 3D7_vir14-3HA was found to the WI-38 lung fibroblasts when compared with the 3D7 parental strain (Fig. 2 *B* and *C*).

A Member of the Pv-FAM-D Multigene Family Has No Direct Role in Cytoadhesion. To determine if members of other multigene families whose expression was also dependent on an intact spleen cytoadhere to spleen fibroblasts, we generated a *P. falciparum* transgenic line (3D7_PvFamD-3HA) expressing a member of the Pv-FAM-D multigene family identified by both algorithms (PVX_101580). Moreover, to avoid confounding, this transgenic line was generated using the same expression vector that the one used to generate the 3D7_vir14-3HA transgenic line (Fig. 3*A*) (23). Expression was validated by RT-PCR (Fig. 3*A*) and indirect immunofluorescence (Fig. 3 *B* and *C*). Colocalization assays with antibodies raised against conserved intracellular acidic terminal segment of PfEMP1 (anti-ATS) revealed that Pv-FAM-D is located at the iRBCs membrane, partially colocalizing with the cytoplasmic domain of PfEMP1 (Fig. 3*B*). Lack of a more punctuated pattern as seen in 3D7 with anti-ATS antibodies (24) is likely due to a different fixation procedure, which gives images similar to those of 3D7 smears fixed with methanol (25). Surface expression was further validated in live immunofluorescence assays (Fig. 3*C*).

Cytoadherence assays showed no significant binding of this transgenic line to human endothelial receptors expressed in CHO cells nor to human Hs 697.Sp or 1010T spleen fibroblasts (Fig. 3 *D* and *E*). A similar or even lower adhesion than the 3D7 parental strain was found. Additionally, a role in adhesion to lung fibroblasts was excluded as no adhesion of the 3D7_PvFamD-3HA transgenic line was observed to WI-38 lung fibroblasts (Fig. 3*E*).

Naturally Acquired Immune Responses of *P. vivax* Spleen-Dependent Antigens. To determine if *P. vivax* spleen-dependent antigens are targets of naturally acquired immune responses, a list of genes for complementary DNA (cDNA) amplification and cloning into the pIVEXGST1.4d vector was selected for expression as glutathione S-transferase (GST)-tagged proteins using the wheat germ in vitro expression system (*SI Appendix*, Table S3) (26). Selection criteria were all members pertaining to subtelomeric multigene families (*vir* and *Pv-fam* genes) by any of the two algorithms used. In addition, we also selected the rest of the genes predicted by the two algorithms, excepting those annotated as enzymes or RNA binding proteins. Unfortunately, despite several different attempts, most of the genes, including PVX_101580, were either unclonable or expressed as insoluble products. Therefore, only five genes representing three different multigene families VIR14 (PVX_108770), Pv-FAM-A (PVX_112670), and Pv-FAM-D (PVX_121910); one membrane transporter SECY (PVX_000960); and one hypothetical protein HYP1 (PVX_114580) were expressed as soluble products in the wheat germ system (*SI Appendix*, Fig. S2) (26). We also expressed a GST-tagged MSP1-19 protein as a control of exposure as this is a highly immunogenic protein in natural vivax infections (27). Immune sera from a retrospective study (28), including 383 children from 1.2 to 5.6 y of age from Papua New Guinea (PNG), were used in multiplex assays as described (26). Recurrence of *P. vivax* in this cohort was high with 91.3 and 76.5% of children

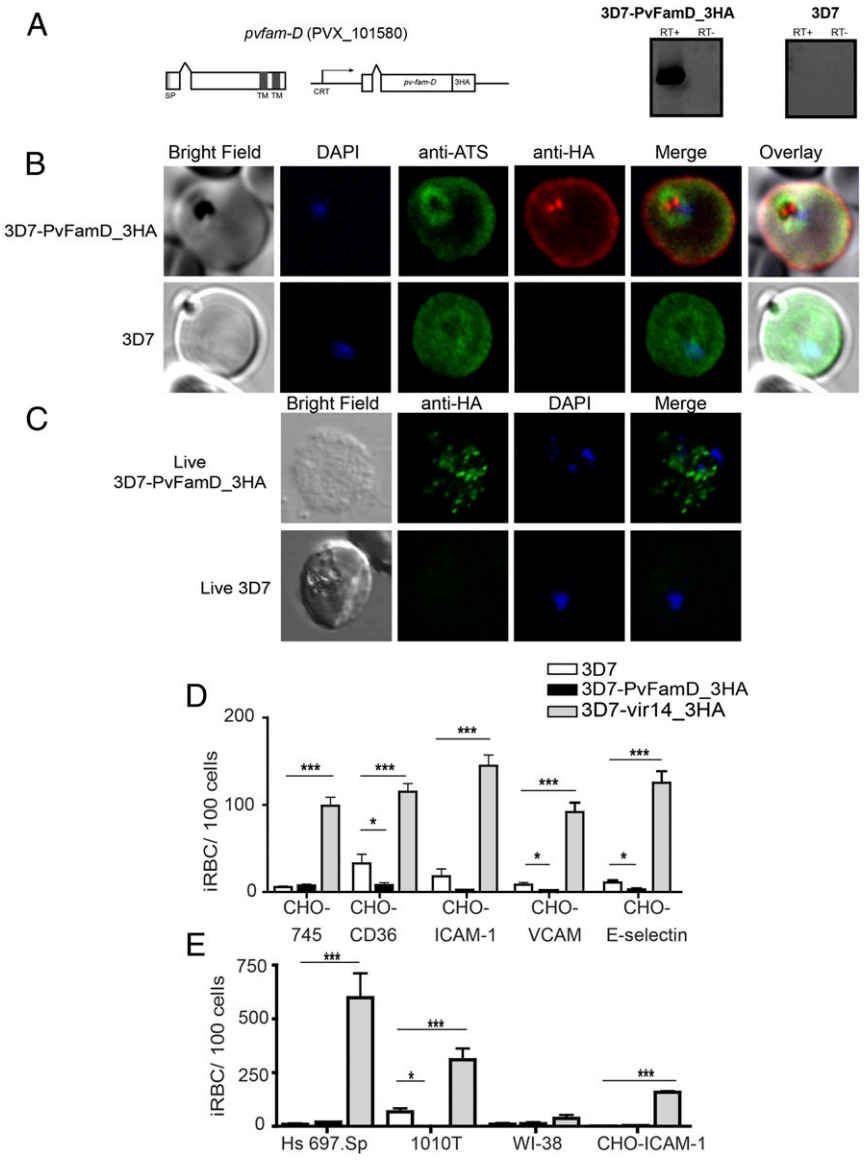

Fig. 3. The multigenic family Pv-FAM-D is expressed in the surface of the *P. falciparum* transgenic line, and it is not implicated into adhesion to endothelial receptors and human spleen and lung fibroblasts. (*A*) Schematic representation of the Pv-FAM-D expression cassette. SP indicates signal peptide, TM indicates transmembrane domain, CRT indicates promoter region of the chloroquine resistance transporter gene, and 3HA indicates triple human influenza hemagglutining tags (*Left*). RT-PCR expression of the *pv-fam-d* gene (*Right*). RT+ indicates cDNA treated with reverse transcriptase, and RT− indicates not treated. (*B*) Coimmunofluorescence images of transgenic strain 3D7_PvFamD-3HA (*Upper*) and 3D7 (*Lower*) labeled with anti-HA (red), anti-ATS (green), and DAPI for nuclear staining. The first column represents differential interference contrast microscopy (DIC), the fifth column represents the merge of the fluorescent staining, and the sixth column represents the overlay of all five images. (*C*) Live immunofluorescence assay. The anti-HA (green) antibody recognized the 3D7_PvFamD-3HA transgenic line and did not recognize the 3D7 parental strain (*Lower*). The first column represents DIC, the third column represents DAPI for nuclear staining, and the fourth column represents the overlay of all images. (*D*) Cytoadherence to CHO cells expressing endothelial receptors. Cytoadherence was expressed as iRBCs per 100 CHO cells. (*E*) Cytoadherence to human fibroblasts (Hs 697.Sp, 1010T, and Wi-38) and CHO-ICAM-1 cells. Significant differences in cytoadhesion are marked with asterisks (unpaired *t* test). Results are shown as the mean of the binding ± SEM of three to five experiments. $*P < 0.05$; $***P < 0.005$.

experiencing a PCR- or light microscopy-detectable *P. vivax* by week 6, respectively (28).

At baseline, 26.4% (HYP1) and 75.6% (VIR14) of children had antibodies to the spleen-dependent antigens, whereas 67.1% of children had antibodies to the nonspleen-dependent MSP1-19 antigen (Fig. 4*A*). Antibodies to PvFAM-D2, SECY, and VIR14 were significantly less commonly observed at week 6 than week 0 ($P < 0.01$) but recovered to pretreatment level at week 40 for PvFAM-D2 and Secy. The prevalence of antibodies to MSP1-19, PvFAM-A2, and HYP1 did not change from week 0 to 6 but decreased significantly by week 40 ($P \leq 0.03$) (Fig. 4*A*). The prevalence of antibodies to VIR14 and HYP1 increased significantly with age ($P \leq 0.002$), indicating continued natural acquisition of immunity (Fig. 4*B*), whereas antibodies to PvFAM-D2 and MSP1-19 were significantly more common in children with concurrent *P. vivax* infections (as detected by light microscopy and/or PCR) (Fig. 4*C*). After adjusting for difference in exposure, children with antibodies against HYP1 (hazard ratio [AHR] = 0.65, confidence interval [CI]95 [0.46, 0.92], $P = 0.01$) showed significant association with protection against clinical

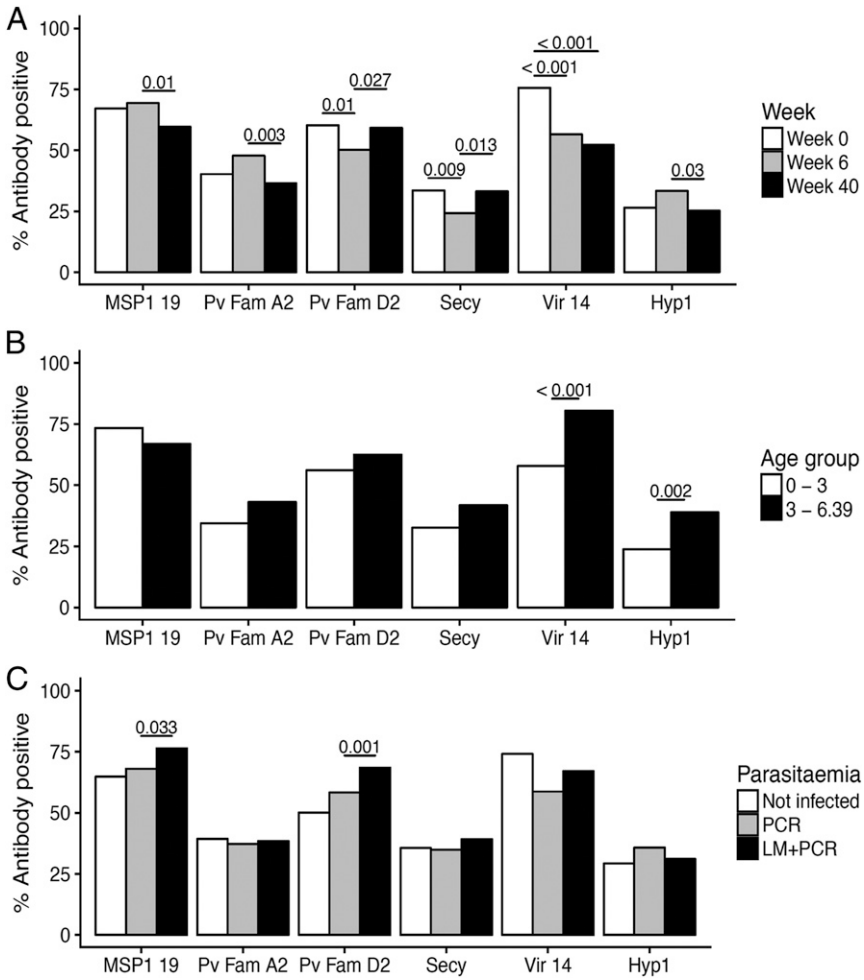

Fig. 4. Prevalence of positive antibody titers according to (*A*) week of follow-up, (*B*) age group cut at median, and (*C*) detectable parasitemia. A positive antibody titer was defined for MFI above mean +2 SD of negative controls. *P* values were adjusted for multiple pairwise comparisons using Tukey's method.

P. vivax episodes during follow-up (*SI Appendix*, Table S4). Children with antibodies to the spleen-dependent PvFAM-D2, however, tended to be at increased risk of acquiring new *P. vivax* during follow-up (light microscopy [LM] positive: AHR = 1.23, CI95 [0.99, 1.52], $P = 0.056$), although not reaching statistical significance. No associations with risk of *P. vivax* infection or disease were observed for antibodies to any of the other antigens.

Discussion

Analysis of infections in splenectomized hosts has demonstrated that the spleen plays a major role in modulating expression of malaria variant multigene families involved in cytoadherence. To understand the role of the spleen in the expression of *P. vivax* genes, we used experimental *P. vivax* infections in splenectomized and spleen-intact *Aotus* monkeys and performed global transcriptional analyses of highly pure and synchronous parasite populations. We demonstrated that 67 coding genes largely located at subtelomeric regions are dependent on the spleen for expression and that such antigens are targets of naturally acquired immune responses.

Several reports based on global transcriptional analysis using customized microarray platforms (29–31), and more recently, on RNA sequencing (RNA-seq), have been applied to sequence *P. vivax* isolates (32–34). These expression data analyses have identified stage-specific and differentially expressed genes coding for proteins with functions related to parasitic development, virulence capacity, and/or host–parasite interaction, among others. We customized an Agilent microarray representing all coding genes of the Salvador I reference strain (10) and identified genes whose expression was dependent on the presence of the spleen in experimental *P. vivax* infections of spleen-intact and splenectomized *Aotus* monkeys. From the 67 spleen-dependent genes identified, close to 50% were located at subtelomeric regions and pertained to variant multigene families (VIR proteins, Pv-FAM-D proteins, Pv-FAM-A proteins, and *Plasmodium* exported proteins) (*SI Appendix*, Table S2). Genes belonging to these multigene families are among the most expressed genes in isolates obtained from different patients, underscoring the importance of variant antigens in natural infections (29–33). Noticeably, gene PVX_108770 (VIR14) pertaining to the *vir* multigene family and shown here to mediate specific cytoadhesion to human spleen fibroblasts was present in the list of 25 *vir* genes highly expressed in clinical isolates (30). Our previous results showed that *P. vivax* VIR proteins present different subcellular localizations revealing that they might play different functions. Additionally, we demonstrated that VIR members of subfamilies A and D do not mediate cytoadherence, whereas VIR14, pertaining to subfamily C, does (23). It is therefore tempting to speculate that spleen-dependent VIR proteins play a role in antigenic variation and cytoadherence in its strict sense, whereas the function of nonspleen-dependent VIR proteins

remains to be elucidated. In the absence of other supporting data, this remains to be determined.

To assess if *P. vivax* spleen-dependent proteins are targets of naturally acquired immune responses, we expressed five genes representing three different multigene families, one membrane transporter, and one hypothetical protein as soluble proteins in the wheat germ cell-free system. This system has proved robust and reproducible to express soluble, mostly intact, and correctly folded malarial proteins (35). Immunogenicity was evaluated measuring total immunoglobin G (IgG) antibody levels of sera from a prospective longitudinal study of children from PNG (28). All proteins were immunogenic, albeit at different levels (Fig. 4) (*SI Appendix*). PvFAM-A2 and PvFAM-D2 proteins were recognized by a high percentage of sera. These results are in agreement with members of these families being highly expressed in transcriptional analysis of parasite isolates (32). Furthermore, a recent study showed that these two members of PvFAM proteins, when analyzed as recombinant proteins using sera from the Republic of Korea (36), were also immunogenic. The fact that antibodies to PvFAM-D2 and MSP1-19 were significantly more common in children with concurrent *P. vivax* infections clearly indicates that these two proteins could be associated with an active infection. Recent analysis of naturally acquired antibody responses to *P. vivax* MSP1-19 in an area of unstable malaria transmission in Southeast Asia has shown that antibodies to $PvMSP1_{19}$ may serve as a serological marker for malaria transmission in that particular study area (37). PvFAM-D2 pertains to a family sharing a conserved N terminus to C terminus protein structure, starting with a signal peptide, followed by Protein Export Elements (PEXEL) motif, antigenic regions containing B cell epitopes, and two transmembrane domains. This topology is only disrupted in two members (PVX_000015 and PVX_118695) where predicted antigenic regions are also observed between the signal peptide and the PEXEL motif (*SI Appendix*, Fig. S3). Further epidemiological studies should determine the value of the Pv-FAM-D family as markers of exposure. On the other hand, low antibody levels were observed against SECY and HYP1. Noticeably, despite pertaining to the variant *vir* gene family with more than a thousand genes described to date, PVX_108770 (VIR14) presented the highest positivity of all antigens tested, including the highly immunogenic MSP1-19 protein. VIR proteins contain predicted immunogenic conserved globular domains of unknown function (9, 23, 38). Whether such domains elicit cross-reacting antibodies responsible for this high percentage of positivity remains to be demonstrated.

The number of genetically distinct blood-stage infections acquired over time, also known as the molecular force of blood-stage infection (molFOB), is a direct way to measure individual differences in exposure to *P. vivax* infections (39). This parameter has also been shown to be a major predictor of clinical disease in *P. falciparum* (40) and vivax malaria (39). Remarkably, when adjusting for difference in exposure, children with antibodies against HYP1 showed significant association with protection against clinical *P. vivax* episodes during follow-up (*SI Appendix*, Table S4). HYP1 is 100% conserved among *P. vivax* isolates from Mauritania, North Korea, India, and Brazil and 90% among other species, including *Plasmodium inui*, *Plasmodium cynomolgi*, *Plasmodium coatneyi*, and *P. knowlesi* (*SI Appendix*, Fig. S4). These results highlight its value as a target for vaccination against asexual blood stages of *P. vivax* and reinforce the importance of using molFOB in the search for association of clinical protection of vaccine candidates in *P. vivax* in prospective longitudinal studies.

P. vivax remains the most widely distributed human malaria parasite. Due to specific biological features, including dormancy in the liver and a tropism for reticulocytes, its elimination requires an improved understanding of its biology and pathogenesis (41). One particular open question regards the conundrum of low peripheral blood parasitemia coincident with severe disease. Recent evidence indicates that this seeming discrepancy could be due to the adherent capacity and sequestration of iRBC parasite populations, outside the peripheral blood, and particularly in the spleen (6, 42–46), the bone marrow (47, 48), and with a less degree of certainty, to other organs (3, 6). Our data thus support a model (Fig. 5) in which infected reticulocytes expressing spleen-dependent VIR proteins, represented here by the VIR14 protein, can adhere to the microvasculature of the spleen, in particular to fibrocytic cells expressing ICAM-1. In contrast, as many VIR proteins are not spleen dependent, it is legitimate to speculate that infected reticulocytes expressing such VIR proteins will not cytoadhere. Therefore, they will circulate in peripheral blood, eliciting the acquisition of cross-reacting VIR antibodies due to the presence of conserved immunogenic globular domains (10, 23, 38) as well as of antibodies against other variant proteins such as PvFAM-D coexpressed in these infected reticulocytes. Further studies of spleen-dependent *P. vivax* genes could thus help in unveiling mechanistic insights of spleen cytoadherence in *P. vivax* as well as discovering new antigens for vaccination and markers of exposure. Most relevant, together with hypnozoite and other tissue reservoirs such as the bone marrow, these populations may represent an added challenge for malaria elimination, particularly since cytoadherence to the microvasculature of the spleen will represent a privileged niche where parasites can escape (46), thus prompting a paradigm shift in *P. vivax* biology toward deeper studies of the spleen during infections.

Materials and Methods

Ethics Statement. The serological analyses of plasma samples from cohort participants received ethical clearance by the PNG Institute of Medical Research Institutional Review Board (IRB; IRB 07.20) and the PNG Medical Advisory Committee (07.34). Individual written consent was obtained from the parents or guardians of all children. The consent included a specific approval to investigate their children's immune responses to different malarial antigens and their association with protection.

The Animal Ethical Committee of Universidad del Valle approved the protocol involving *Aotus lemurinus griseimebra* monkeys from the Fundacion Centro de Primates in Cali, Colombia. Animals were handled and housed following the National Research Council's *Guide for the Care and Use of Laboratory Animals* (50).

Infections of *Aotus* Monkeys. Five groups of *A. lemurinus griseimebra* monkeys ($n = 2$ per group), four splenectomized (Sp−1, Sp−2, Sp−3, and Sp−4) and one with spleen (Sp+2), were used. All groups were handled according with animal welfare guidelines and maintained with standard requirements of water and food supplies. Animals were splenectomized by a veterinarian according to standard operational procedures under general anesthesia 4 wk prior to infections.

Spleen-intact (Sp+) and splenectomized (Sp−) animals were infected by intravenous (iv) inoculation of 10^5 iRBCs (500-μL volume) obtained from a donor monkey previously infected with the *P. vivax* Sal-1 reference strain (10). First recipient group was splenectomized monkeys (Sp−1 group); thereafter, parasites were passaged by iv inoculations through groups Sp−2, Sp−3, Sp−4, and Sp+2. Parasite passages were performed at peak parasitemia (~3 to 4 wk postinoculation); simultaneously, 3 to 4 mL of peripheral blood was collected via femoral vein in heparinized sterile tubes from each animal, and 1-mL aliquots were processed for RNA extractions.

Sample Processing for RNA Isolation and Gene Expression Array. For RNA isolation, blood was first centrifuged at 600 × *g* for 5 min, and packed RBCs were resuspended at 25% hematocrit in incomplete Roswell Park Memorial Institute medium (iRPMI). Mature *P. vivax* parasites were purified using magnetic MACS LS columns (Miltenyi) as described (51) and preserved into 1 mL of TRIzol for later processing. RNA extraction was performed following the manufacturer's instructions, and 50 ng of each sample was reversely transcribed into cDNA, being subsequently amplified and labeled with Cy5 and Cy3 dye following Agilent's Two-Color Microarray-Based Gene

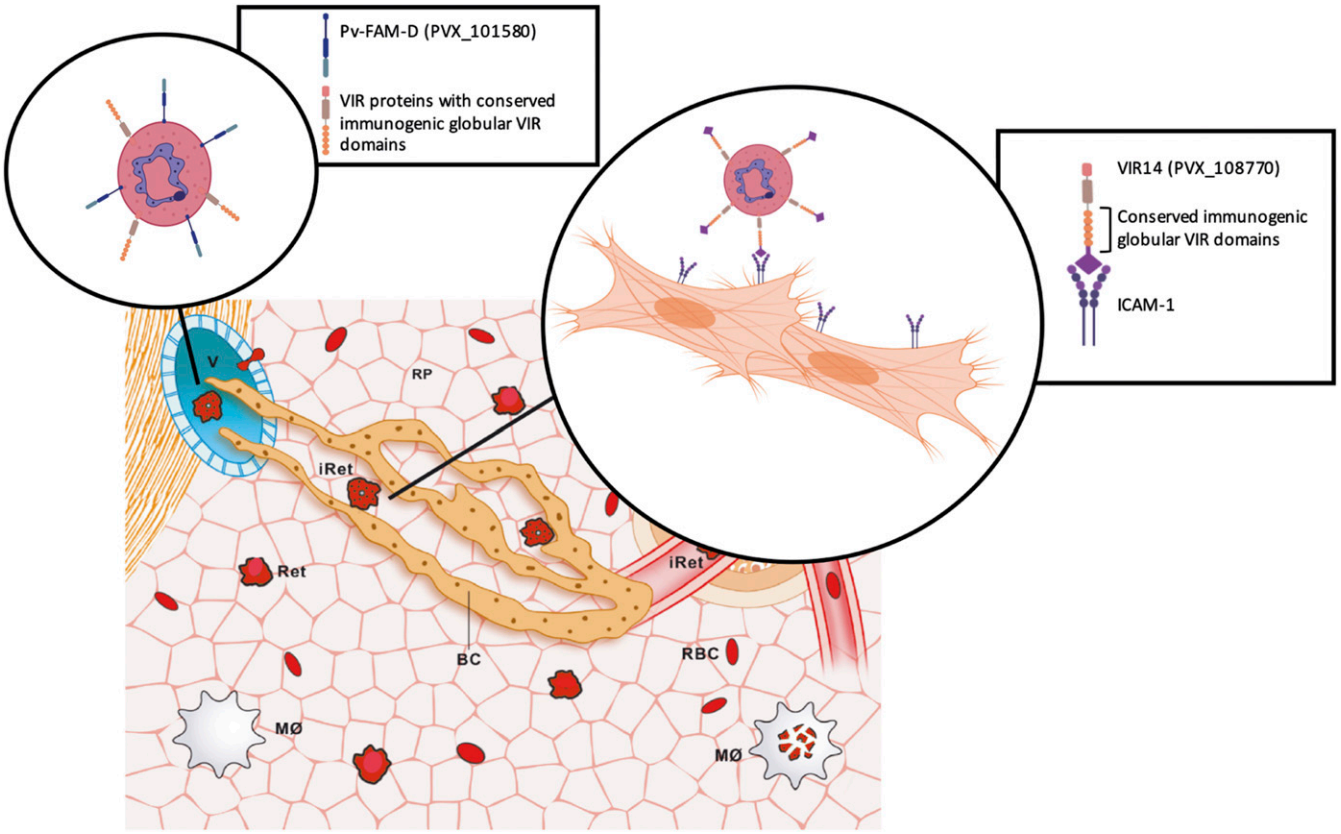

Fig. 5. Spleen cytoadherence mediated by spleen-dependent VIR proteins. Infections by reticulocyte (Ret)-prone malaria parasites induce spleen remodeling and formation of barrier cells (BCs) of fibroblastic origin where infected reticulocytes (iRets) avoid macrophage (MO) clearance (background scheme) (49). *P. vivax* iRets expressing spleen-dependent VIR proteins, here represented by VIR14 (PVX_108770), adhere to human spleen fibroblasts expressing ICAM-1 (*Right Inset*). iRets expressing VIR proteins whose expression is not spleen-dependent will not cytoadhere; thus, reaching peripheral circulation facilitating antigen presentation of conserved immunogenic VIR globular domains (10, 23, 38) as well as other variant antigens such as PvFAM-D (PVX_101580; *Left Inset*). Partially created by BioRender. RP, red pulp; V, venule.

Expression Analysis protocol version 6.5 (Agilent Technologies). Spike-in RNA (Agilent Technologies) was used as internal control. Slides were scanned with Agilent's G2565CA Microarray Scanner System. Dye normalized, background subtracted, and log ratios of sample to reference expression were calculated using Agilent's Feature Extraction Software version 9.5.

Dual hybridizations comparing the global expression of parasites obtained from the different experimental infections (labeled with Cy5) with a reference pool PvSp-1 obtained from splenectomized monkeys from the CDC (donated by John Barnwell; labeled with Cy3) were performed using Agilent's custom-made array containing 5,038 *P. vivax* coding genes (one 60-base oligonucleotide at every 2 kb) as annotated (10). Of note, sample Sp−4 was not included in these analyses due to insufficient amount of total RNA obtained. All data are freely available through the GEO NIH database repository (GEO accession no. GPL6667).

Selection of Spleen-Dependent Genes Based on Microarray Analyses. Two distinct probabilistic models were proposed to identify *P. vivax* genes expressed only in monkeys with intact spleen (*SI Appendix*, Fig. S1), one considering each time point independently (Method 1) and the other considering the entire time series (Method 2). In the first model, probe intensities were compared with negative controls. Each negative control was considered as a realization of a random variable (I_{ctrl}), and a probability density function was modeled using straightforward Kernel Density Estimation (52) in R programming language's package stats (53). Average intensity of each gene probe (a number, I_{probe}) was compared with the probability density function of the negative controls. If the negative control would rarely generate intensity signals greater than what was observed for a given probe, we say that this probe is expressed (on). Formally, if $Pr(I_{ctrl} > I_{probe}) < 0.001$, then probe is on. Conversely, if negative control could easily generate similar intensity levels that gene probes also can, we say that this probe is not confidently expressed (off). Formally, if $Pr(I_{ctrl} > I_{probe}) > 0.05$, then probe is off. In the second model, a 0.98 quantile of negative control intensity was used as a cutoff. Probes presenting average intensity at least 10 times greater than this cutoff were considered on, and the ones with average intensity below the quantile were classified as off. For each model, selected genes were those presenting the following expression pattern: off in Sp−1, Sp−2, and Sp−3 and on in Sp+2. Intrinsic variability of the log ratio and mean average plot in the different arrays limited the possibility of performing a robust differential *vir* gene expression analysis.

Fibroblasts and CHO Cells Culture. The spleen fibroblast cell line (1010T) was established in our laboratory from a human spleen donated by the Hospital Clinic of Barcelona in accordance with the protocol approved by the Ethics Committee for Clinical Research of the Universitat de Barcelona (no. 041499). Briefly, a portion of the spleen was fragmented into several parts and divided into two tubes to be homogenized by the GentleMACS dissociator. After applying the "Spleen 1" program twice, the sample was centrifuged at 700 × *g* for 10 min. The obtained pellet was resuspended in complete RPMI supplemented with 10% fetal bovine serum (FBS) (cRPMI) at a final density of 10^8 cells in 30 mL of medium and cultured at 37 °C/5% CO_2. After 2 d, the cell suspension was removed, and only adherent cells were kept in culture for 3 to 4 wk until 100% of confluence was reached before trypsinization.

CHO cells were grown in cRPMI medium, while the commercial fibroblasts Hs 697.Sp (ATCC CRL-7433) and WI-38 (ATCC CCL-75) were cultured in complete Dulbecco's Modified Eagle Medium (supplemented with 10% FBS serum). All cell cultures were maintained at 37 °C/5% CO_2.

***P. falciparum* Static and Flow Cytoadhesion Assays.** Static binding assays were performed as previously described (23). Briefly, 5×10^4 CHO cells (CHO-746, CHO-CD36, CHO-ICAM-1, CHO-VCAM, and CHO-E-Selectine (donated by Artur Scherf, Biology of Host-Parasites Interactions, Institut Pasteur, Paris, France) were seeded in 24-well plates in coverslips (Nunc) and left to attach

for 2 d. Half of the content of a 75-cm^2 flask of Hs697 Sp, 1010T, and WI-38 cell lines was used to seed 12 wells. In the case of the Hs697 cell line, the cells were seeded 5 d before performing the experiment. Mature asexual blood stages of cultured *P. falciparum* 3D7 strain and the transgenic lines were enriched using a 70% Percoll solution, and parasites were quantified using both a Neubauer chamber and a Giemsa-stained smear. For adhesion experiments, cells were washed with binding medium (RPMI, pH 6.8 supplemented with 10% AB^+ human plasma), and 500 μL containing 1×10^6 *P. falciparum* transgenic parasites were added to each well. Each experiment was run in triplicate. Cells and iRBCs were incubated for 1 h at 37 °C in binding medium in a 5% CO_2 incubator, and unbound cells were washed by dipping coverslips twice in binding medium followed by 30 min of gravity wash at a 45° angle. Adhesion experiments with the WI-38 cell line were done in binding medium at a pH of 7.2 to avoid cell clumping. The same medium was used for experiments run in parallel with WI-38, CHO-ICAM-1, and Hs697 Sp cells. For flow cytoadhesion assays, coverslips seeded with either CHO or Hs 697Sp cell lines were mounted in a Cell Adhesion Flow Chamber. The system was connected to a precise infusion/withdrawal pump (model KDS120; KD Scientific) to control the flow of the iRBC suspension through the perfusion chamber; then, 1×10^7 iRBCs were flowed over for a total of 30 min, and binding buffer was flowed over for 10 min to remove unbound cells. The flow rate yielded a wall shear stress of 0.09 Pa, which mimics wall shear stresses in the microvasculature. Static and flow coverslips were fixed in methanol after the washing process and stained with 10% Giemsa for 15 min. Adhesions were quantified in an optical light microscope. Binding experiments were done in triplicate in 3 to 5 independent days. Statistical analysis was done on GraphPad Prism (version 4), and significance was determined by an unpaired *t* test.

***P. falciparum* Culture, Plasmid Constructs, and Parasite Transfection.** *P. falciparum* parasites were cultured with B+ human erythrocytes (3% hematocrit) in RPMI media (Sigma) supplemented with 10% AB+ human plasma using standard methods (23). *Pv-fam-d* gene (PVX_101580) was amplified from *P. vivax* Sal1 genomic DNA (gDNA) using primers F-PvfamD: GGTACCATGAAA ATGAAAAAAAATAAG; R-PvfamD: ctgcagATTTCTTGGTCTTTTTTTTG and was cloned in the KpnI-PstI cloning sites of modified transfection vector pARL1a-3HA (23). The plasmid pARL1a-PvfamD-3HA was transfected into 3D7 parasites by electroporating ring-stage parasites (>5% parasitemia) with 100 μg of purified plasmid DNA (Qiagen) as previously described (23) using 0.310-kV and 950-F electroporation conditions. Six hours after transfection, 2.5 nM WR99210 was added to the culture media. Parasites were detectable in culture 20 to 30 d after drug selection pressure started.

***P. falciparum* Indirect Immunofluorescence Assays.** Cultured *P. falciparum* 3D7-Pv-fam-D_3HA transgenic line that presents mixed stages was washed in phosphate-buffered saline (PBS) and then fixed with 4% electron microscopy (EM)-grade paraformaldehyde and 0.075% EM-grade glutaraldehyde in PBS (23). Fixed cells were permeabilized with 0.1% Triton X-100 in PBS and blocked for 1 h at room temperature in 3% PBS-bovine serum albumin (BSA). Samples were incubated overnight with primary antibody (rabbit anti-HA [1:50; Molecular Probes] or rat anti-HA [1:50; Roche] and mouse anti-ATS [1:50]) diluted in 3% PBS-BSA followed by 1 h of incubation with secondary antibody (anti-mouse or anti-rat IgG conjugated with Alexa Fluor 488 and anti-rabbit IgG conjugated with Alexa Fluor 594 [1:100; Molecular Probes]) diluted in 3% PBS-BSA. Nuclei were stained in the secondary antibody incubation with 4,6-diaminido-2-phenylindole (DAPI; 2 mg/mL diluted in 3% PBS-BSA). Confocal microscopy was performed using a laser-scanning confocal microscope (TCS-SP5; Leica Microsystems) at microscopy scientific and technical services of Universitat de Barcelona. Images were processed using ImageJ image browser software.

***P. falciparum* Live Immunofluorescence Assays.** Cultured *P. falciparum* transgenic lines were washed in iRPMI and blocked for 1 h at room temperature in 3% RPMI-BSA (PBS-BSA). Samples were incubated for 1 h with rabbit anti-HA (1:50; Molecular Probes) diluted in 3% RPMI-BSA followed by 1 h of incubation with secondary antibody anti-rabbit IgG conjugated with Alexa Fluor 488 (1:100; Molecular Probes) diluted in RPMI. Nuclei were stained in the secondary antibody incubation with DAPI (2 mg/mL). Samples were mounted in Vectashield (Vector Labs), and confocal microscopy was performed using a laser-scanning confocal microscope (TCS-SP5; Leica Microsystems). Images were processed using ImageJ image browser software.

Cloning and Small-Scale Wheat Germ Cell-Free Protein Synthesis. *P. vivax* spleen-dependent genes were amplified from cDNA (Sal-1 strain) by PCR using Platinum Taq DNA Polymerase High Fidelity (Thermo Ficher Scientific) and the primers listed in *SI Appendix*, Table S5. PCR products were initially cloned into pGEM-T easy vector (Promega) and subcloned into pIVEX1.4d vector (Roche), previously modified by our group, by inserting GST after the 6xHis tag sequence (26). Authenticity of all clones encoding GST-fusion proteins was confirmed by sequencing before expression in the wheat germ cell-free system (Roche). In vitro protein synthesis was done on a 50-μL scale as described (26) and purified on GST SpinTrap purification columns (GE Healthcare). GST was also expressed separately for immunereactivity control.

Antibody Measurement by Luminex Technology. For antibody measurement, 1 μg of each recombinant protein was covalently coated to different MagPlex magnetic carboxylated microspheres (Luminex Corporation) following the manufacturer's instructions. Measurement of total IgG antibodies was performed by multiplex suspension array using the Luminex technology as previously described (54). Briefly, a batch of microspheres, containing 2,000 beads per analyte, was incubated with human plasma samples (1:100 dilution) in duplicates and subsequently, with anti-human IgG biotinylated (Sigma-Aldrich) at 1:4,000 dilution followed by streptavidin-conjugated R-phycoerthrin (R-PE) (1 μg/mL). Beads were acquired on the BioPlex100 system (Bio-Rad), and results are expressed as median fluorescence intensity. A panel of eight negative controls was included on every plate.

Antibodies to all proteins were measured in a cohort of PNG children aged 1 to 5 y enrolled in a longitudinal cohort study who were randomized to pretreatment with artesunate (7 d), artesunate (7 d) plus primaquine (14 d), or no treatment and followed up actively for recurrent *Plasmodium* infections and disease for 40 wk. A detailed description of the cohort is given elsewhere (28). Antibodies were measured in samples collected at baseline (n = 435), 6 wk after treatment (n = 408), and at the end of follow-up (n = 419). Antibody mean fluorescent intensities (MFIs) were log transformed, and background values due to antibody reactivity to the GST tag were subtracted as described (54). Cutoffs for antibody positivity were determined for each plate separately by calculating mean +2 SD of the negative control values.

Statistical Analysis. Clinical malaria was defined as fever (axillary temperature ≥37.5 °C) or recent history of febrile illness and presence of a concomitant *Plasmodium* sp. infection. Time at risk was counted from the first day after the last treatment dose was administered and up until withdrawal, loss to follow-up, or study completion. Associations between the time to first *Plasmodium* sp. infection (or clinical episode) and treatment options were already investigated in a previous study (28) and relied on Cox proportional hazard regressions using Schoenfeld residuals test to confirm the proportional hazard assumption. In this study, we also included recoded antibody titers as explanatory independent covariates in these regressions.

Recoding of Antibody Titers. To account for plate-to-plate variations and to reflect on antibody level, MFIs were adjusted, platewise, under the assumption that log(Ab_tag) ~ log(Ab) + log(tag). A linear model was fitted to each plate and antigen to derive the adjusted MFI value: the minimal tag value that could be detected was hence considered as background noise from the experiment.

Adjusted MFI values from negative controls were used to define a standard reference curve, reflecting the expected values of cross-reactivity that could be expected in individuals who were never exposed to *Plasmodium* parasites. Assuming log-normal distributions of MFI values in this control population, extreme outliers were flagged using Grubb's test recursively (55).

Positivity thresholds were defined plate- and antigenwise as 2 SDs above the mean MFI in negative controls. Patients' adjusted MFIs values were compared against these thresholds and recoded to binomial outcomes (positive/negative). As a sensitivity analysis, a more conservative set of thresholds was computed using 3 SDs.

Logistic regression was used to quantify the associations between baseline positivity and age categories (two groups cut at a median of 3 y old), *Plasmodium* sp. parasitemia, and clinical episodes, while adjusting for the averaged individual molecular force of infection as a proxy for individual exposure to mosquitoes. Temporal trends in prevalence of antibody positivity were estimated using generalized estimating equations with exchangeable correlation structure to account for repeated measurements.

ACKNOWLEDGMENTS. We thank John Barnwell (Malaria Branch, Division of Parasitic Diseases and Malaria, CDC) for the gift of the reference RNA pool PvSp-1 obtained from splenectomized monkeys from the CDC, Artur Scherf (Biology of Host-Parasite Interactions, Institut Pasteur) for the gift of CHO-cells expressing different receptors and Marc Nicolau for technical assistance.

We also thank the anonymous reviewers of this manuscript whose criticisms and suggestions significantly improved its content and quality. This work was supported with funding from the Cellex Foundation. The funder had no role in study design, data collection and analysis, decision to publish, or preparation of the manuscript. The Barcelona Institute for Global Health (ISGlobal) receives support from the Spanish Ministry of Science, Innovation and Universities through the "Centro de Excelencia Severo Ochoa 2019-2023" Program (CEX2018-000806-S). This research is part of ISGlobal's Program on the Molecular Mechanisms of Malaria, which is partially supported by the Fundación Ramón Areces. ISGlobal and Germans Trias i Pujol Research Institute are members of the Centres de Reserca de Catalunya Program, Generalitat de Catalunya.

1. R. E. Howes *et al*., Global epidemiology of *Plasmodium vivax*. *Am. J. Trop. Med. Hyg.* **95** (suppl. 6), 15–34 (2016).
2. J. K. Baird, Neglect of *Plasmodium vivax* malaria. *Trends Parasitol.* **23**, 533–539 (2007).
3. M. V. Lacerda *et al*., Postmortem characterization of patients with clinical diagnosis of *Plasmodium vivax* malaria: To what extent does this parasite kill? *Clin. Infect. Dis.* **55**, e67–e74 (2012).
4. C. Naing, M. A. Whittaker, V. Nyunt Wai, J. W. Mak, Is *Plasmodium vivax* malaria a severe malaria?: A systematic review and meta-analysis. *PLoS Negl. Trop. Dis.* **8**, e3071 (2014).
5. L. H. Miller, D. I. Baruch, K. Marsh, O. K. Doumbo, The pathogenic basis of malaria. *Nature* **415**, 673–679 (2002).
6. B. O. Carvalho *et al*., On the cytoadhesion of *Plasmodium vivax*-infected erythrocytes. *J. Infect. Dis.* **202**, 638–647 (2010).
7. K. Chotivanich *et al*., Plasmodium vivax adherence to placental glycosaminoglycans. *PLoS One* **7**, e34509 (2012).
8. B. De las Salas *et al*., Adherence to human lung microvascular endothelial cells (HMVEC-L) of *Plasmodium vivax* isolates from Colombia. *Malar. J.* **12**, 347 (2013).
9. H. A. del Portillo *et al*., A superfamily of variant genes encoded in the subtelomeric region of *Plasmodium vivax*. *Nature* **410**, 839–842 (2001).
10. J. M. Carlton *et al*., Comparative genomics of the neglected human malaria parasite *Plasmodium vivax*. *Nature* **455**, 757–763 (2008).
11. H. A. Del Portillo *et al*., The role of the spleen in malaria. *Cell. Microbiol.* **14**, 343–355 (2012).
12. C. R. Engwerda, L. Beattie, F. H. Amante, The importance of the spleen in malaria. *Trends Parasitol.* **21**, 75–80 (2005).
13. J. W. Barnwell, R. J. Howard, L. H. Miller, Altered expression of *Plasmodium knowlesi* variant antigen on the erythrocyte membrane in splenectomized rhesus monkeys. *J. Immunol.* **128**, 224–226 (1982).
14. S. A. Lapp *et al*., Spleen-dependent regulation of antigenic variation in malaria parasites: *Plasmodium knowlesi* SICAvar expression profiles in splenic and asplenic hosts. *PLoS One* **8**, e78014 (2013).
15. M. Hommel, P. H. David, L. D. Oligino, Surface alterations of erythrocytes in *Plasmodium falciparum* malaria. Antigenic variation, antigenic diversity, and the role of the spleen. *J. Exp. Med.* **157**, 1137–1148 (1983).
16. S. M. Handunnetti, K. N. Mendis, P. H. David, Antigenic variation of cloned *Plasmodium fragile* in its natural host *Macaca sinica*. Sequential appearance of successive variant antigenic types. *J. Exp. Med.* **165**, 1269–1283 (1987).
17. C. F. Gilks, D. Walliker, C. I. Newbold, Relationships between sequestration, antigenic variation and chronic parasitism in *Plasmodium chabaudi* chabaudi—a rodent malaria model. *Parasite Immunol.* **12**, 45–64 (1990).
18. M. Demar, E. Legrand, D. Hommel, P. Esterre, B. Carme, *Plasmodium falciparum* malaria in splenectomized patients: Two case reports in French Guiana and a literature review. *Am. J. Trop. Med. Hyg.* **71**, 290–293 (2004).
19. A. Bachmann *et al*., Absence of erythrocyte sequestration and lack of multicopy gene family expression in *Plasmodium falciparum* from a splenectomized malaria patient. *PLoS One* **4**, e7459 (2009).
20. S. Looareesuwan, P. Suntharasamai, H. K. Webster, M. Ho, Malaria in splenectomized patients: Report of four cases and review. *Clin. Infect. Dis.* **16**, 361–366 (1993).
21. K. Chotivanich *et al*., Parasite multiplication potential and the severity of Falciparum malaria. *J. Infect. Dis.* **181**, 1206–1209 (2000).
22. C. Fernandez-Becerra *et al*., *Plasmodium vivax* and the importance of the subtelomeric multigene vir superfamily. *Trends Parasitol.* **25**, 44–51 (2009).
23. M. Bernabeu *et al*., Functional analysis of *Plasmodium vivax* VIR proteins reveals different subcellular localizations and cytoadherence to the ICAM-1 endothelial receptor. *Cell. Microbiol.* **14**, 386–400 (2012).
24. A. G. Maier *et al*., Skeleton-binding protein 1 functions at the parasitophorous vacuole membrane to traffic PfEMP1 to the *Plasmodium falciparum*-infected erythrocyte surface. *Blood* **109**, 1289–1297 (2007).
25. V. Kumar *et al*., PHISTc protein family members localize to different subcellular organelles and bind *Plasmodium falciparum* major virulence factor PfEMP-1. *FEBS J.* **285**, 294–312 (2018).
26. E. Rui *et al*., *Plasmodium vivax*: Comparison of immunogenicity among proteins expressed in the cell-free systems of *Escherichia coli* and wheat germ by suspension array assays. *Malar. J.* **10**, 192 (2011).
27. P. A. Nogueira *et al*., A reduced risk of infection with *Plasmodium vivax* and clinical protection against malaria are associated with antibodies against the N terminus but not the C terminus of merozoite surface protein 1. *Infect. Immun.* **74**, 2726–2733 (2006).
28. I. Betuela *et al*., Relapses contribute significantly to the risk of *Plasmodium vivax* infection and disease in Papua New Guinean children 1-5 years of age. *J. Infect. Dis.* **206**, 1771–1780 (2012).
29. S. J. Westenberger *et al*., A systems-based analysis of *Plasmodium vivax* lifecycle transcription from human to mosquito. *PLoS Negl. Trop. Dis.* **4**, e653 (2010).
30. Z. Bozdech *et al*., The transcriptome of *Plasmodium vivax* reveals divergence and diversity of transcriptional regulation in malaria parasites. *Proc. Natl. Acad. Sci. U.S.A.* **105**, 16290–16295 (2008).
31. P. A. Boopathi *et al*., Revealing natural antisense transcripts from *Plasmodium vivax* isolates: Evidence of genome regulation in complicated malaria. *Infect. Genet. Evol.* **20**, 428–443 (2013).
32. A. Kim *et al*., Characterization of *P. vivax* blood stage transcriptomes from field isolates reveals similarities among infections and complex gene isoforms. *Sci. Rep.* **7**, 7761 (2017).
33. L. Zhu *et al*., New insights into the *Plasmodium vivax* transcriptome using RNA-Seq. *Sci. Rep.* **6**, 20498 (2016).
34. A. Kim, J. Popovici, D. Menard, D. Serre, *Plasmodium vivax* transcriptomes reveal stage-specific chloroquine response and differential regulation of male and female gametocytes. *Nat. Commun.* **10**, 371 (2019).
35. T. Tsuboi, S. Takeo, T. U. Arumugam, H. Otsuki, M. Torii, The wheat germ cell-free protein synthesis system: A key tool for novel malaria vaccine candidate discovery. *Acta Trop.* **114**, 171–176 (2010).
36. F. Lu *et al*., Profiling the humoral immune responses to *Plasmodium vivax* infection and identification of candidate immunogenic rhoptry-associated membrane antigen (RAMA). *J. Proteomics* **102**, 66–82 (2014).
37. Q. Wang *et al*., Naturally acquired antibody responses to *Plasmodium vivax* and *Plasmodium falciparum* Merozoite Surface Protein 1 (MSP1) C-terminal 19 kDa domains in an area of unstable malaria transmission in Southeast Asia. *PLoS One* **11**, e0151900 (2016).
38. P. Requena *et al*., *Plasmodium vivax* VIR proteins are targets of naturally-acquired antibody and T cell immune responses to malaria in pregnant women. *PLoS Negl. Trop. Dis.* **10**, e0005009 (2016).
39. C. Koepfli *et al*., A high force of *Plasmodium vivax* blood-stage infection drives the rapid acquisition of immunity in Papua New Guinean children. *PLoS Negl. Trop. Dis.* **7**, e2403 (2013).
40. I. Mueller *et al*., Force of infection is key to understanding the epidemiology of *Plasmodium falciparum* malaria in Papua New Guinean children. *Proc. Natl. Acad. Sci. U.S.A.* **109**, 10030–10035 (2012).
41. I. Mueller *et al*., Key gaps in the knowledge of *Plasmodium vivax*, a neglected human malaria parasite. *Lancet Infect. Dis.* **9**, 555–566 (2009).
42. J. K. Baird, Evidence and implications of mortality associated with acute *Plasmodium vivax* malaria. *Clin. Microbiol. Rev.* **26**, 36–57 (2013).
43. A. Machado Siqueira *et al*., Spleen rupture in a case of untreated *Plasmodium vivax* infection. *PLoS Negl. Trop. Dis.* **6**, e1934 (2012).
44. M. S. Peterson *et al*.; MaHPIC Consortium, *Plasmodium vivax* parasite load is associated with histopathology in *Saimiri boliviensis* with findings comparable to *P vivax* pathogenesis in humans. *Open Forum Infect. Dis.* **6**, ofz021 (2019).
45. A. Elizalde-Torrent *et al*., Sudden spleen rupture in a *Plasmodium vivax*-infected patient undergoing malaria treatment. *Malar. J.* **17**, 79 (2018).
46. R. S. Lee, A. P. Waters, J. M. Brewer, A cryptic cycle in haematopoietic niches promotes initiation of malaria transmission and evasion of chemotherapy. *Nat. Commun.* **9**, 1689 (2018).
47. B. Baro *et al*., *Plasmodium vivax* gametocytes in the bone marrow of an acute malaria patient and changes in the erythroid miRNA profile. *PLoS Negl. Trop. Dis.* **11**, e0005365 (2017).
48. N. Obaldia 3rd *et al*., Bone marrow is a major parasite reservoir in *Plasmodium vivax* infection. *MBio* **9**, e00625-18 (2018).
49. L. Martin-Jaular *et al*., Strain-specific spleen remodelling in *Plasmodium yoelii* infections in Balb/c mice facilitates adherence and spleen macrophage-clearance escape. *Cell. Microbiol.* **13**, 109–122 (2011).
50. National Research Council, *Guide for the Care and Use of Laboratory Animals*, (National Academies Press, Washington, DC, ed. 8, 2011).
51. D. T. Trang, N. T. Huy, T. Kariu, K. Tajima, K. Kamei, One-step concentration of malarial parasite-infected red blood cells and removal of contaminating white blood cells. *Malar. J.* **3**, 7 (2004).
52. B. W. Silverman, *Density Estimation*, (Chapman and Hall, London, UK, 1986).
53. R Core Team, *R: A Language and Environment for Statistical Computing*, (R Foundation for Statistical Computing, Vienna, Austria, 2015).
54. C. Fernandez-Becerra *et al*., Naturally-acquired humoral immune responses against the N- and C-termini of the *Plasmodium vivax* MSP1 protein in endemic regions of Brazil and Papua New Guinea using a multiplex assay. *Malar. J.* **9**, 29 (2010).
55. F. E. Grubbs, Sample criteria for testing outlying observations. *Ann. Math. Stat.* **21**, 27–58 (1950).